

# Thermotropic polyesters: structure of poly(chloro-1,4-phenylene terephthalate) and its copolymers

D. J. Johnson, I. Karacan, P. E. P. Maj\* and J. G. Tomka†

Textile Physics Laboratory, Department of Textile Industries, University of Leeds, Leeds LS2 9JT, UK

(Received 20 July 1989; revised 20 November 1989; accepted 23 February 1990)

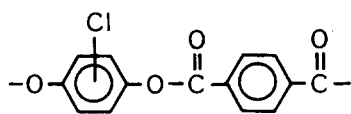
Structures of poly(chloro-1,4-phenylene terephthalate) and two series of nematogenic copolymers with reduced chain rigidity, viz. poly(chloro-1,4-phenylene terephthalate-co-4,4'-oxybisbenzoate)s containing an ether oxygen disruptor, and poly(chloro-1,4-phenylene terephthalate-co-4,4'-hexamethylenedioxybisbenzoate)s containing a hexamethylenedioxy flexible spacer, are investigated by wide-angle X-ray techniques. The chain packing density in crystals of the parent rigid-chain 'homopolymer' is similar to those of unsubstituted polyesters containing 1,4-phenylene moieties. In contrast, the parent 'homopolymers' of reduced chain rigidity have crystal structures with increased interchain spacings. Copolymers with the ether oxygen disruptor contain crystallites of the less rigid parent 'homopolymer' while those with the flexible spacer contain crystallites of both parent 'homopolymers'. This is attributed to the combined effects of chain cross-sectional areas and melting temperatures of the parent 'homopolymers'.

(Keywords: aromatic polyesters; thermotropic; nematic; liquid crystalline; X-ray diffraction)

## INTRODUCTION

Rigid-chain polyesters, such as poly(1,4-phenylene terephthalate) and poly(4-oxybenzoate), are not suitable for melt processing due to their high melting temperatures (above 600°C). Modifications of their chemical structure by the introduction of substituents, angular or crankshaft disruptors or flexible spacers, result in melt-processable nematogenic materials<sup>1-3</sup>. Initially, research concerned with thermotropic nematogenic polymers concentrated on the relationships between chemical structure and transition temperatures, but now there is a growing emphasis on characterization of physical structure<sup>4,5</sup>.

The effect of substitution on the crystal-nematic transition temperature,  $T_{CN}$ , of poly(1,4-phenylene terephthalate) is well documented; the lowering of  $T_{CN}$  depends on the size of the substituent, its location and the degree of substitution<sup>3,6</sup>. Replacement of a single hydrogen atom in the hydroquinone moiety by chlorine does not result in a sufficient lowering of  $T_{CN}$  for successful melt processing. Thus, the  $T_{CN}$  of poly(chloro-1,4-phenylene terephthalate) (PCPT; repeat unit I)



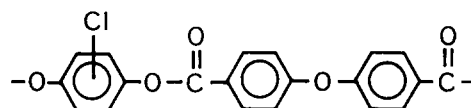
I CPT

is 340–370°C, which is still too high<sup>7</sup>. Although this material is referred to as a homopolymer, the relative

locations of the chlorine atoms in successive repeat units may differ and are not specified. It is likely that the PCPT chains consist of a random sequence of units substituted in 2 and 3 positions of the hydroquinone moieties. This also applies to other polymers containing chlorohydroquinone moieties.

Although further reduction of  $T_{CN}$  can be achieved by increasing the size of the substituent or by placing an additional substituent on the terephthaloyl moiety<sup>6</sup>, we have pursued a different but well established<sup>1,2</sup> approach, based on modifications of chain rigidity<sup>7-9</sup>.

Poly(chloro-1,4-phenylene 4,4'-oxybisbenzoate) (PCPO; repeat unit II)



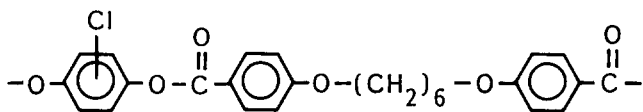
II CPO

and poly(chloro-1,4-phenylene terephthalate-co-4,4'-oxybisbenzoate)s (PCPT-co-CPO), containing an ether oxygen angular disruptor, are nematogenic, but only copolymers with molar fractions of disruptor units ([CPO]) ranging from 0.25 to 0.75 are melt processable<sup>7</sup>. At room temperature the mechanical properties of mouldings and heat-treated fibres produced from copolymer [CPO] = 0.50 are satisfactory, although not outstanding. However, a significant reduction of stiffness takes place at elevated temperatures. This is due to a mechanical loss process occurring around 120°C and associated with the glass transition<sup>8</sup>.

\* Present address: ATOCHEM, 27470 Serquigny, France

† To whom correspondence should be addressed

Poly(chloro-1,4-phenylene 4,4'-hexamethylenedioxybisbenzoate) (PCPH; repeat unit III)



III CPH

and poly(chloro-1,4-phenylene terephthalate-co-4,4'-hexamethylenedioxybisbenzoate)s (PCPT-co-CPH), containing hexamethylenedioxy flexible spacer, are also nematogenic throughout the whole composition range<sup>9</sup>. The transition of these solid copolymers into nematic melts is a complex process involving melting of two types of ordered regions. The properties of fibres and mouldings produced from the copolymer with molar fraction of spacer units [CPH]=0.50 are much worse than those of the corresponding material containing the ether oxygen disruptor<sup>9</sup>.

This paper is concerned with structural characterization of these materials, particularly the more promising copolymers PCPT-co-CPO, by wide-angle X-ray techniques. The main emphasis is placed on the evaluation of the chain cross-sectional areas in the crystals. Where chain folding does not occur, the differences between the attainable lateral chain packing densities are expected to affect the relative stabilities of the crystallites, which consist of repeat units of individual parent homopolymers.

## EXPERIMENTAL

The polymers and fibres were the same as those used previously<sup>7-9</sup>; their wide-angle X-ray diffraction patterns were taken with a flat-plate camera, and diffractometer traces ( $2\theta$  range between 10 and 35°) were obtained with a modified Hilger and Watts Y115 diffractometer. The correction and normalization procedures as well as the data processing methods were described previously<sup>10</sup>.

## RESULTS AND DISCUSSION

### Poly(chloro-1,4-phenylene terephthalate)

Since poly(chloro-1,4-phenylene terephthalate) (PCPT) could not be melt spun, only unoriented 'as-made' material has been investigated. Its wide-angle X-ray photograph indicates the presence of a crystalline structure. The diffractometer trace (Figure 1c) shows at least seven peaks in the  $2\theta$  range between 10 and 35°, but an acceptable peak resolution required at least two additional peaks. The  $d$ -spacings of all nine resolved peaks are listed in Table 1 together with their relative peak areas. The diffraction pattern obtained here differs in several respects from that reported by Krigbaum *et al.*<sup>6</sup>, which contained six reflections. Five of Krigbaum's reflections had  $d$ -spacings similar to those found here (cf. Table 1), although the intensities are somewhat different; the sixth very strong reflection had a  $d$ -spacing of 0.723 nm. These authors did not record a reflection corresponding to our prominent peak 2 ( $d=0.529$  nm). The reason for this discrepancy is unknown, but it should be noted that our material was prepared in the absence of catalyst<sup>7</sup>, while Krigbaum *et al.*<sup>6</sup> used 0.01% of magnesium.

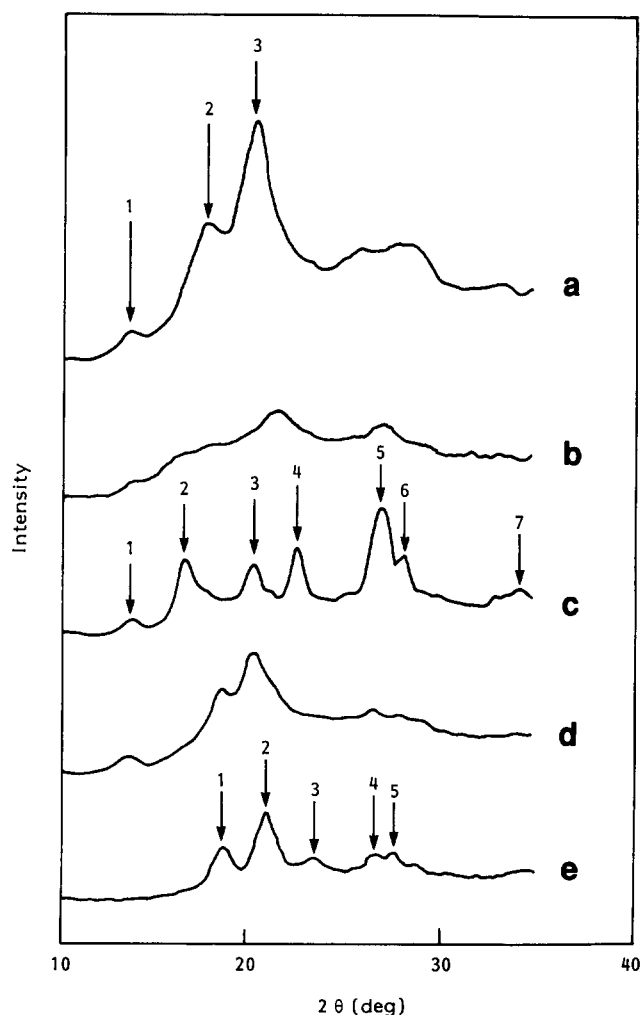


Figure 1 Diffractometer traces of (a) PCPO; (b) PCPT-co-CPO, [CPO]=0.50; (c) PCPT; (d) PCPT-co-CPH, [CPH]=0.50; (e) PCPH

Table 1 X-ray reflections of poly(chloro-1,4-phenylene terephthalate) (PCPT): assignment and calculated  $d$ -spacings for orthorhombic unit cell given in Table 2

$h k l$	Peak <sup>a</sup>	$d_{\text{obs}}$ (nm)	$d_{\text{calc}}$ (nm)	$A_{\text{rel}}^d$
0 1 0	2	0.529	0.527	0.77
1 1 0	3	0.437 <sup>c</sup>	0.438	1.00
2 0 0	4	0.394 <sup>c</sup>	0.394	0.83
0 2 0	7	0.264	0.264	0.21
0 0 2	1	0.628	0.631	0.03
1 0 2	<sup>b</sup>	0.495	0.493	0.30
1 1 2	<sup>b</sup>	0.354 <sup>c</sup>	0.360	0.13
2 0 2	5	0.332 <sup>c</sup>	0.334	1.48
0 0 4	6	0.317 <sup>c</sup>	0.316	0.64

<sup>a</sup> See Figure 1c

<sup>b</sup> Additional peaks obtained after resolution

<sup>c</sup> Reflections observed by Krigbaum *et al.*<sup>6</sup>

<sup>d</sup> Relative peak areas, taking peak 3 (1 1 0) as the reference

The small number of reflections, together with the unavailability of a well oriented specimen, would normally make the task of gaining information about the crystal structure of PCPT impossible. However, Coulter *et al.*<sup>11</sup> recently carried out an investigation of the crystal structure of the corresponding unsubstituted polyester, poly(1,4-phenylene terephthalate) (PPT), using powder X-ray diffraction data in conjunction with molecular

**Table 2** Crystal structures of aromatic polymers:  $d$ -spacings of the main equatorial reflections ( $h+k \leq 2$ ) and their relative intensities; unit-cell dimensions; chain cross-sectional areas  $Q_c$ 

Polymer	$d$ (nm)				Unit cell <sup>a</sup>			$Q_c$ (nm <sup>2</sup> )	Ref.
	0 1 0	1 1 0	2 0 0	0 2 0	$a$ (nm)	$b$ (nm)	$c$ (nm)		
PPT	–	0.442 (vs)	0.394 (s)	–	0.798	0.533	1.264	0.210	11
POB	0.570 (s)	0.454 (vs)	0.376 (vs)	0.285 (w)	0.752	0.570	1.249	0.214	13
PPTA	–	0.433 (vs)	0.394 (vs)	0.259 (vw)	0.787	0.518	1.290	0.204	12
PPO	–	0.457 (vs)	0.404 (vs)	0.277	0.807	0.554	0.972	0.224	14
PEK	–	0.470 (vs)	0.382 (s)	–	0.763	0.596	1.000	0.227	15
PEEK	–	0.467 (vs)	0.388 (s)	–	0.775	0.586	1.000	0.227	15
PPS	–	0.471 (s)	0.434 (vs)	0.281 (w)	0.867	0.561	1.026	0.243	16
PCPT	0.529 (vs)	0.437 (vs)	0.394 (vs)	0.265 (vw)	0.788	0.527	1.262	0.208	–

<sup>a</sup> Containing two chains; orthorhombic, except PPT, which is monoclinic with  $\gamma = 99^\circ$

Polymer abbreviations:

PPT poly(1,4-phenylene terephthalate)

POB poly(4-oxybenzoate)

PPTA poly(1,4-phenylene terephthalamide)

PPO poly(phenylene oxide), i.e. poly(oxy-1,4-phenylene)

PEK poly(aryl ether ketone), i.e. poly(oxy-1,4-phenylene-carbonyl-1,4-phenylene)

PEEK poly(aryl ether ether ketone), i.e. poly(oxy-1,4-phenylene-oxy-1,4-phenylene-carbonyl-1,4-phenylene)

PPS poly(phenylene sulphide), i.e. poly(thio-1,4-phenylene)

PCPT poly(chloro-1,4-phenylene terephthalate)

modelling. The unit cell proposed for the low-temperature structure of PPT is monoclinic with orthogonal lateral chain packing. Except for the axial displacement of the chains, the unit cell is similar to the pseudo-orthorhombic cell of the corresponding polyamide, poly(1,4-phenylene terephthalamide) (PPTA)<sup>12</sup>. Indeed, inspection of published data<sup>12–16</sup> on several aromatic polymers consisting solely of 1,4-phenylene moieties linked by various groups indicates that orthorhombic (or pseudo-orthorhombic) structure is typical for such materials (Table 2).

The  $d$ -spacings of the prominent PCPT peaks 3 and 4 (Table 1) are very close to those of the 1 1 0 and 2 0 0 reflections of PPT and PPTA (Table 2). This similarity led to the tentative indexing of PCPT reflections in terms of an orthorhombic unit cell with the dimensions given in Table 2. An attempt to introduce a 'monoclinic shear' as used by Coulter *et al.*<sup>11</sup> resulted in a poorer match between the observed and calculated  $d$ -spacings.

Unlike PPT and PPTA, PCPT shows a very strong 0 1 0 reflection; this indicates that its space group differs from those of the corresponding unsubstituted polymers. However, owing to the small number of observed reflections, no attempt has been made to characterize the structure of PCPT in detail.

The main conclusion resulting from the investigation of PCPT concerns its chain cross-sectional area. It is found that, within the limit of experimental error, it is identical with those of unsubstituted aromatic polyesters and PPTA, i.e. about 0.21 nm<sup>2</sup> (Table 2). This shows that, surprisingly, the effect of the chlorine substituent on the chain packing density in the crystal lattice is negligible.

#### Poly(chloro-1,4-phenylene 4,4'-oxybisbenzoate)

Comparison of the diffractometer traces (Figures 1a

and 1c) shows that the crystal structure of poly(chloro-1,4-phenylene 4,4'-oxybisbenzoate) (PCPO) differs from that of PCPT. The trace of the 'as-made' PCPO shows three discrete peaks in the  $2\theta$  range between 10 and 23° (Table 3). The scatter in the  $2\theta$  range between 24 and 30° suggests the presence of at least two further peaks, but these cannot be resolved reliably.

Melt spinning of PCPO proved to be difficult and only a poorly oriented fibre was obtained. Its X-ray diffraction pattern shows only two equatorial and one off-equatorial reflection (Table 3). The two strong reflections found in the 'as-made' polymer are close to the equatorial reflections of the fibre and thus originate from the lateral packing of PCPO chains. Their  $d$ -spacings (Table 3) are significantly larger than those arising from interchain distances in PCPT and this indicates a much poorer lateral packing of PCPO chains compared with PCPT.

Data in Table 2 show that the chain cross-sectional areas of polymers containing angular linkages (–O–, –CO–, –S–) are larger than those found for the polymers where the outgoing bonds of the linking groups are nearly parallel (–COO–, –CONH–). It is also noted that a decrease of the bond angle of the angular linkage (from 124° for –O– to 110° for –S–), causing an increase in the angle between the chain axis and that of 1,4-phenylene groups (from 28° to 35°), results in an increase of the chain cross-sectional area. Obviously, the presence of the angular ether oxygen in PCPO (Figure 2) is responsible for increased interchain spacings in this polymer compared with PCPT.

The repeat length of the fully extended planar conformation of PCPO (Figure 2), calculated as 3.48 nm, contains two chemical repeat units. The angle between the chain axis and the axes of 1,4-phenylene groups attached to the ether oxygen (labelled as Ph3 and Ph4) is the same as in poly(1,4-phenylene oxide) (PPO).

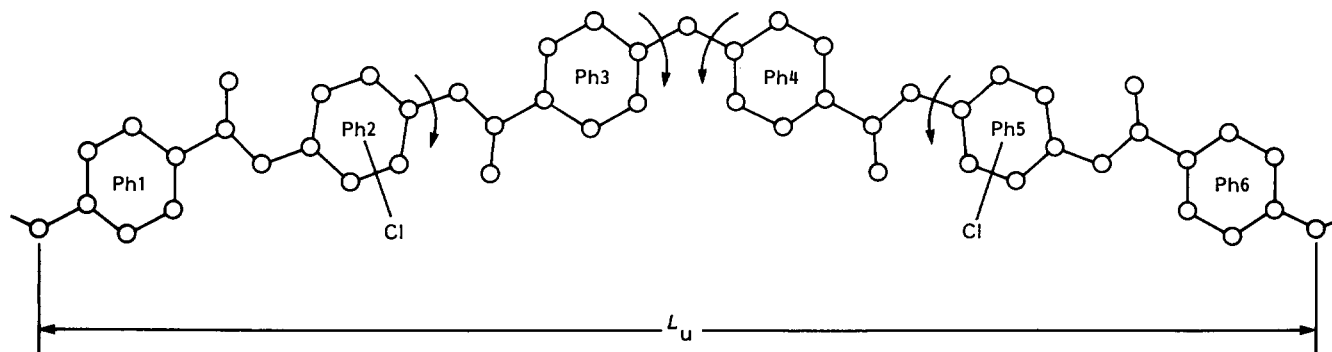


Figure 2 Fully extended planar chain conformation of poly(chloro-1,4-phenylene 4,4'-oxybisbenzoate) (PCPO)

Table 3 Prominent wide-angle X-ray reflections in poly(chloro-1,4-phenylene 4,4'-oxybisbenzoate) (PCPO) and in poly(chloro-1,4-phenylene terephthalate-co-4,4'-oxybisbenzoate)s (PCPT-co-CPO): *d*-spacings (nm)

Type	PCPO		PCPT-co-CPO	
	Polymer	Fibre	Polymer <sup>a</sup>	Fibres <sup>b</sup>
–	0.637	–	–	–
Equatorial	0.497	0.504	0.496	0.487–0.493
Equatorial	0.436	0.429	0.425	0.430–0.435
Off-equatorial	–	0.330	–	0.331–0.333

<sup>a</sup> [CPO]=0.50; annealed for 10 min at 250°C

<sup>b</sup> Range of values for 'as-made' and heat-treated fibres, [CPO]=0.40, 0.50, 0.60 and 0.75

Notwithstanding the rotations of the chloro-1,4-phenylene rings (Ph2 and Ph5) arising from steric interference with ester groups, there is an additional complication due to the steric interaction due to the steric interaction between aromatic rings Ph3 and Ph4 adjacent to the ether oxygen. Investigation of the structure of poly(1,4-phenylene oxide) showed<sup>14</sup> that the torsion angles of these aromatic rings are approximately  $\pm 40^\circ$ . If the ester groups in PCPO remained essentially coplanar with Ph3 and Ph4 rings, this out-of-plane rotation would result in a non-planar conformation with a shortened repeat length and increased cross-sectional area.

#### *Poly(chloro-1,4-phenylene terephthalate-co-4,4'-oxybisbenzoate)s*

The diffractometer traces of PCPT-co-CPO 'as-made' copolymers with molar fractions of disruptor units containing ether oxygen [CPO] ranging from 0.25 to 0.75 showed only a few rather broad reflections, and it was therefore impossible to decide whether the ordered regions in these materials are similar to those present in either of the parent 'homopolymers'. This is illustrated by the trace of copolymer [CPO]=0.50 shown in Figure 1b. However, after a short annealing (10 min at 250°C), distinct reflections appeared with *d*-spacings similar to those found in PCPO (Table 3).

'As-made' fibre produced from [CPO]=0.50 copolymer by melt spinning from the nematic mesophase using a drawdown ratio of approximately 40 was highly oriented (Figure 3). It showed features assigned to the PCPO structure, i.e. two prominent equatorial reflections (Figure 4, peaks C1 and C2) with *d*-spacings similar to those found for the annealed copolymer (Table 3), as well as the off-equatorial reflection with a *d*-spacing of

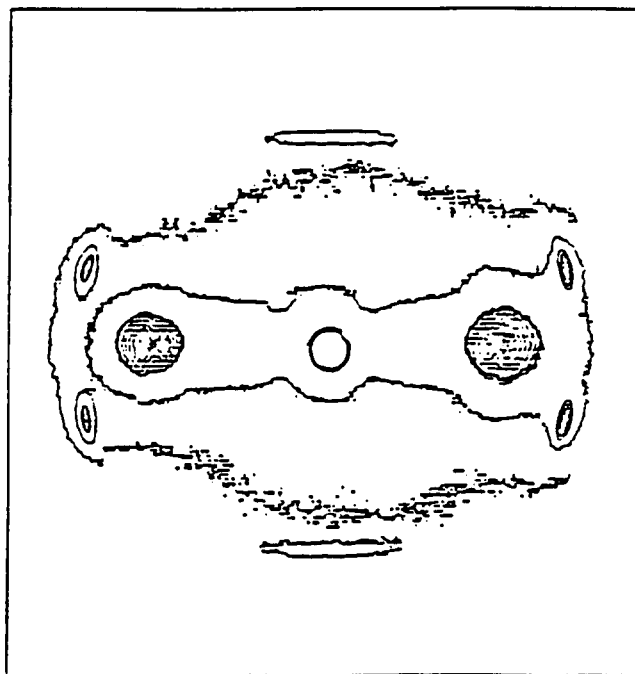


Figure 3 Wide-angle X-ray contour map of 'as-made' PCPT-co-CPO, [CPO]=0.50 fibre. Fibre axis is vertical

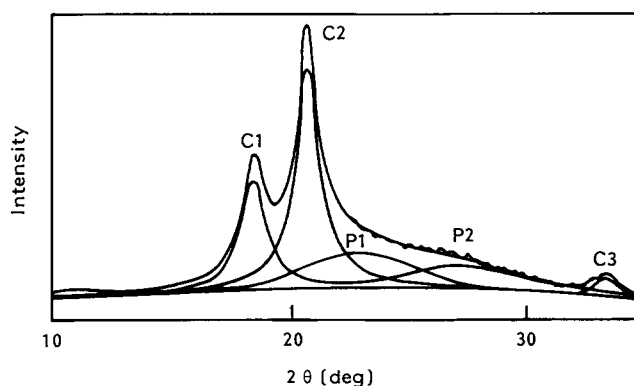
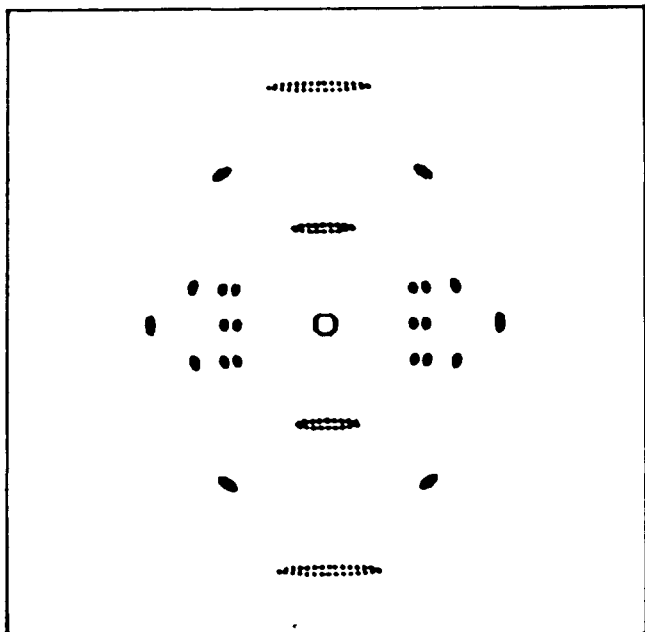


Figure 4 Resolved equatorial X-ray diffraction trace of 'as-made' PCPT-co-CPO fibre, [CPO]=0.50. For *d*-spacings see Table 5

0.331 nm, arced around a 1.15 nm layer line. There was also an additional equatorial reflection with a *d*-spacing of 0.272 nm (Figure 4, peak C3). Overexposed X-ray film showed additional very weak layer line reflections, shown schematically in Figure 5 and listed in Table 4. These



**Figure 5** Schematic diagram of an X-ray diffraction pattern of highly oriented PCPT-*co*-CPO fibres. The meridional streaks are attributed to the non-crystalline matrix

**Table 4** Crystalline structure of PCPT-*co*-CPO fibres ([CPO]  $\geq$  0.40): mean values of observed *d*-spacings in comparison with those calculated for an orthogonal chain packing with  $a=0.980$  nm and  $b=0.481$  nm

Location	<i>h k l</i>	<i>d</i> -spacing (nm)	
		Obs.	Calc.
Equator	2 0 0	0.490 (vs)	0.490
	1 1 0	0.432 (vs)	0.432
	3 1 0	0.272 (m)	0.270
1.15 nm layer line	2 0 -	0.453 (vw)	-
	1 1 -	0.409 (vw)	-
	2 1 -	0.333 (vs)	-
0.31 nm layer line	1 1 -	0.253 (vw)	-

very weak reflections and the additional equatorial reflection were assigned to the PCPO crystalline structure. The only feature found on the meridian was a weak horizontal streak with a *d*-spacing of 0.419 nm (Figure 3); an additional streak with a *d*-spacing of 0.213 nm was revealed after tilting. Such streaks are qualitatively different from the arced equatorial and off-equatorial reflections assigned to the crystalline structure. They are typical of a parallel array of chains without long-range order of lateral packing<sup>5</sup>. The streaks, together with the diffuse equatorial scatter in the  $2\theta$  range between 22 and 32° (Figure 4), are assigned to the non-crystalline matrix.

The structure of 'as-made' fibres produced from copolymers [CPO]=0.40 and 0.60 at drawdown ratios greater than 35 was very similar to that of the [CPO]=0.50 fibre. Prolonged heat treatments of [CPO]=0.40 and 0.50 fibres did not result in significant changes of crystal structure. Spinning of copolymer [CPO]=0.75 proved to be difficult and only much smaller drawdown ratios could be achieved. Nevertheless, even in these less well oriented fibres the PCPO crystalline structure was present. Thus, elongational flow

taking place during the spinning of PCPT-*co*-CPO copolymers with [CPO]  $\geq$  0.40 results in formation of crystalline structure similar to that found in the PCPO 'homopolymer'; subsequent heat treatment does not affect the structure formed during spinning from the nematic mesophase.

Using the reflections listed in Table 4, an attempt was made to evaluate the lateral chain packing in PCPO crystals present in highly oriented PCPT-*co*-CPO fibres. Since meridional reflections arising from PCPO crystalline structure are absent and the number of layer line reflections is small, it was impossible to evaluate the unit-cell type and the crystal repeat length in the chain direction. Assuming an orthogonal packing in the *ab* plane and provisionally indexing the equatorial reflections in descending order of *d*-spacings as 1 1 0, 2 0 0 and 0 2 0 (i.e. in accordance with the results for other aromatic polymers listed in Table 2), we did not get a satisfactory solution. However, by reversing the provisional indexing of the prominent equatorial reflections (see Table 4) it was possible to assign the reflections to an orthogonal packing with  $a=0.980$  nm and  $b=0.481$  nm. The off-equatorial reflections are located on row lines corresponding to this packing. Although the obtained *a* and *b* values appear to be unrelated to those reported for other aromatic polymers (Table 2), the differences in chain packing are actually rather small, as shown by broken lines in Figure 6, where the distances A'C (0.872 nm) and A'A (0.546 nm) correspond to *a* and *b* dimensions of other aromatic polymers. However, this alternative arrangement is not orthogonal ( $\gamma \approx 98^\circ$ ).

The chain cross-sectional area for the proposed PCPO lateral chain packing is 0.236 nm<sup>2</sup>, i.e. larger than those found for PPO, PEK and PEEK but smaller than that of PPS (Table 2). It exceeds the value obtained for PCPT

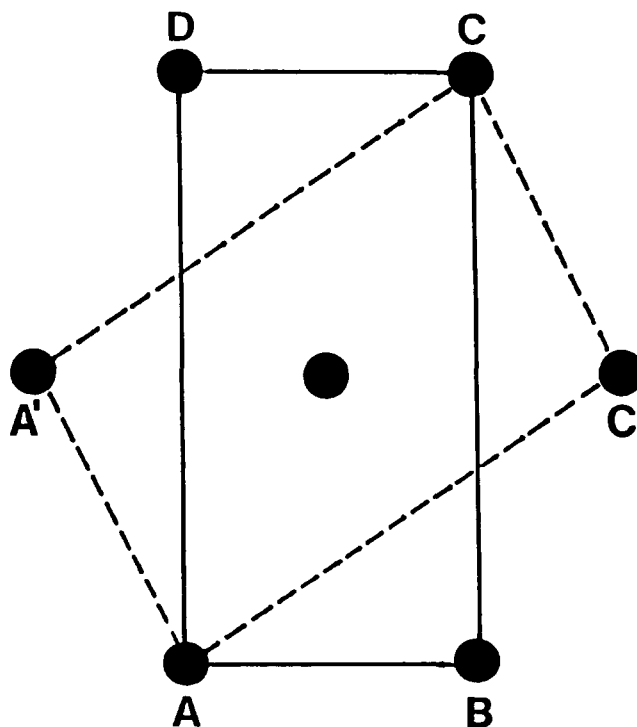


**Figure 6** Orthorhombic chain packing in PCPO (ABCD); alternative interpretation (A'AC'C) is related to the chain packing in other aromatic polymers (Table 2)

by about 13%. The significance of this difference for the formation of the PCPO crystallites in PCPT-*co*-CPO copolymers will be discussed later.

#### Structure of PCPT-*co*-CPO fibres

The dominant features of the equatorial scatter of PCPT-*co*-CPO fibres ( $[\text{CPO}] \geq 0.40$ ) are three sharp peaks (C1, C2 and C3) arising from crystalline regions with the PCPO structure; but there is also additional scatter in the  $2\theta$  range between  $22$  and  $32^\circ$ , which is assigned to the non-crystalline matrix. This is illustrated in Figure 4, which shows the diffractometer trace for the  $[\text{CPO}] = 0.50$  'as-made' fibre. An acceptable resolution of this trace was obtained with two additional broad peaks, P1 and P2, arising from the non-crystalline matrix. Data obtained from the trace resolution are summarized in Table 5. It should be noted that the  $d$ -spacing of the peak P1 is close to that of the prominent 2 0 0 reflection of PCPT. As already mentioned, the horizontal meridional streaks are also ascribed to this non-crystalline matrix consisting of chain segments with a high degree of alignment along the fibre axis. We refer to this type of structure as paracrystalline<sup>10</sup>, although the use of this term is sometimes met with scepticism. The fractional peak areas given in Table 5 are related to the total area of all five peaks. However, the total fractional area under the crystalline peaks C1–C3 ( $A_c$ ) cannot be used as a measure of crystallinity since another broad peak (related to the 1 1 0 reflection of PCPT) may be hidden under the peak C2. Nevertheless, the values of  $A_c$  can be used for assessment of structural changes resulting from heat treatment.

The apparent lateral dimensions of PCPO crystallites calculated from the width of the resolved equatorial peaks C1 and C2 are also listed in Table 5. It is estimated that the crystallites contain more than 100 laterally packed chains. Unfortunately, in the absence of meridional reflections arising from the PCPO structure, we are unable to evaluate the crystallite dimension in the chain direction.

In the absence of reflections arising from crystal planes perpendicular to the chain axis, it is possible to evaluate the orientation factor of the crystallites ( $f_c$ ) from the azimuthal spread of equatorial reflections; for an orthogonal chain packing, two such reflections are sufficient<sup>17</sup>. Here, the crystallite orientation was evaluated from the azimuthal scans of the prominent 2 0 0 and 1 1 0 reflections. Since the crystallite size in the chain direction is not known, the correction for this effect could not be applied. The uncorrected value of  $f_c$  is 0.97, but the actual value would be even higher. Thus, the alignment of the axes of the PCPO crystallites along the fibre axis is almost perfect.

**Table 5** 'As-made' PCPT-*co*-CPO fibre ( $[\text{CPO}] = 0.50$ ): equatorial features

Peak	C1	C2	C3	P1	P2
<i>h k l</i>	2 0 0	1 1 0	3 1 0	–	–
$d$ -spacing (nm)	0.488	0.434	0.272	0.394	0.332
Peak width at half-height (deg)	1.24	1.12	1.12	5.23	5.46
Apparent crystal size (nm)	5.9	6.1	–	–	–
Relative area	0.21	0.41	0.02	0.19	0.17
Azimuthal peak width at half-height (deg)	7.80	7.30	–	–	–

**Table 6** Effect of copolymer composition ( $[\text{CPO}]$ ) and heat treatment at  $230^\circ\text{C}$  on the structure of PCPT-*co*-CPO fibres:  $A_c$  = total fractional area of the crystalline peaks C1–C3;  $L$  = apparent crystal size;  $f_c$  = orientation factor of the crystallites

$[\text{CPO}]$	Heat treatment (min)	$A_c$	$L$ (nm)		$f_c$
			2 0 0	1 1 0	
0.40	None	0.62	6.0	6.3	0.96
	2 4 0	0.57	5.9	6.5	–
	4 8 0	0.68	6.3	7.0	0.98
0.50	None	0.64	5.9	6.1	0.97
	1 2 0	0.61	6.2	7.0	–
	2 4 0	0.60	6.1	7.3	0.97
0.60	None	0.61	6.0	6.4	0.96

**Table 7** Wide-angle X-ray reflections in poly(chloro-1,4-phenylene 4,4'-hexamethylenedioxybisbenzoate) (PCPH)

Peak	<i>h k l</i>	$d$ -spacing (nm)
1	2 0 0	0.476
2	1 1 0	0.425
3	–	0.379
4	2 1 0	0.336
5	–	0.325

Data presented in Table 6 show that neither the changes in copolymer composition ( $[\text{CPO}]$  between 0.40 and 0.60) nor the heat treatment substantially affect the structure of PCPT-*co*-CPO fibres. Hence, the observed improvements of tensile strength resulting from the prolonged heat treatments of the 'as-made' PCPT-*co*-CPO fibres must be attributed to the rise of molecular weight<sup>8</sup>.

It should be noted that the behaviour of PCPT-*co*-CPO fibres (i.e. the lack of structural differences arising from heat treatment or from variations in copolymer composition) is in contrast with the behaviour of poly(*p*-oxybenzoate-*co*-*p*-phenylene isophthalate) fibres spun from a nematic mesophase. There, the structure was strongly influenced by both the copolymer composition and the heat treatment conditions<sup>10</sup>. There are therefore at least two different types of behaviour concerning the development of crystal structure in thermotropic nematogenic copolymers.

#### Poly(chloro-1,4-phenylene 4,4'-hexamethylenedioxybisbenzoate) and its copolymers

Only a cursory investigation of the structure of these materials has been carried out. The diffractometer trace of the unoriented 'as-made' PCPH homopolymer (Figure 1e) shows two prominent peaks and at least three other peaks; their  $d$ -spacings are given in Table 7. From comparison with the trace of PCPT (Figure 1c) it is obvious that the crystal structures of these 'homopolymers' are different (see Tables 1 and 7). Assuming an orthogonal packing of PCPH chains and indexing the prominent reflections (peaks 1 and 2) as in PCPO, we get  $a = 0.952$  nm and  $b = 0.475$  nm; peak 3 is then indexed as 2 1 0 (Table 7). The estimated chain cross-sectional area of PCPH ( $0.226$  nm<sup>2</sup>) is smaller than that of PCPO ( $0.236$  nm<sup>2</sup>) but significantly exceeds the value obtained for PCPT ( $0.208$  nm<sup>2</sup>). Since the cross-sectional area of the aliphatic spacer with extended *trans* conformation should be smaller than that of the aromatic sequence in

PCPH, this result suggests that the aliphatic spacer is not fully extended. Similar behaviour has been observed for other polymers containing aliphatic spacers<sup>18</sup>. The cross-sectional area obtained for the PCPH chain is actually close to that of the hexagonal phase in polyethylene<sup>19</sup>.

The diffractometer trace of PCPT-*co*-CPH 'as-made' copolymer with a molar fraction of spacer units [CPH]=0.50 (Figure 1d) shows peaks 1 and 3 of the PCPT structure as well as peak 1 of the PCPH structure. The shoulder in the  $2\theta$  range 16–18° yields, after trace resolution, a peak with *d*-spacing close to that of PCPT peak 2. The trace resolution also gives an additional peak related to PCPH peak 2 (see Table 8). It is concluded that this copolymer contains crystal structures of both parent 'homopolymers'.

This also applies to copolymers with [CPH]=0.25 and 0.75 (Table 8). Figure 7 shows that the relative area of PCPT peak 2 decreases with increasing concentration of spacer units, while the opposite is true for PCPH peak 1. The WAXS evidence is essentially in agreement with the conclusions based on investigation of the melting behaviour of PCPT-*co*-CPH copolymers<sup>9</sup>. However, the resolved trace of copolymer [CPH]=0.25 indicated the presence of PCPH crystallites, although the endotherm arising from their melting has not been detected.

#### The role of chain cross-sectional areas in crystallization of nematogenic copolymers

The relative stabilities of crystalline phases in a binary mixture of low-molecular-weight compounds A and B are expressed by the well known Schroeder–Van Laar relationship. Thus, the stability of a crystalline phase A is determined by the composition of the mixture together with the equilibrium melting point ( $T_{m,A}^{\circ}$ ) and the molar enthalpy of fusion ( $\Delta H_{m,A}^{\circ}$ ) of the pure compound A. In random copolymers, consisting of repeat units A and B, the situation is far more complex<sup>20</sup>. Since macroscopic phase separation cannot take place, the interfacial energies become important. In flexible-chain polymers and copolymers, the end surface free energies ( $\gamma_e$ ) of crystallites are large due to the energy of chain folding. In main-chain nematogenic copolymers, the absence of chain folding results in much smaller end surface energies. This, according to Blundell<sup>21</sup>, explains why unusually small crystallites may be formed in such copolymers. We suggest that in these copolymers the values of  $\gamma_e$  are influenced by the mismatch between the cross-sectional

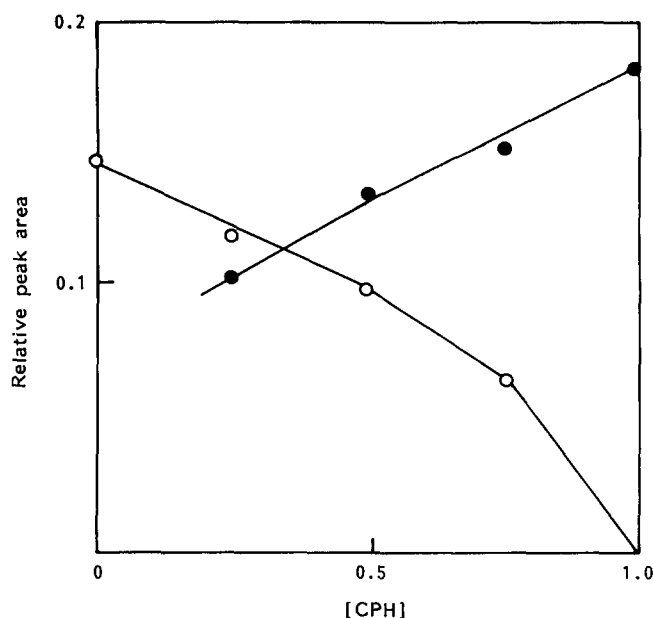


Figure 7 Effect of the molar fraction of spacer units [CPH] in PCPT-*co*-CPH copolymers on relative peak areas of (○) PCPT, peak 2 and (●) PCPH, peak 1

areas of the units forming the crystallites and those emerging from the crystallites. If the chain cross-sectional area of the units incorporated into the crystallites is smaller than that of the units emerging from the end surface of the crystallite, the value of  $\gamma_e$  is increased due to the steric 'overcrowding' at the interface.

At this stage we do not have the thermodynamic data required for a quantitative analysis (i.e. the appropriate equilibrium melting temperatures and heats of fusion). However, the consideration of chain cross-sectional areas qualitatively explains the crystallization behaviour of the copolymers investigated.

In the case of PCPT-*co*-CPO copolymers, the observed melting temperatures of the two parent 'homopolymers' are similar ( $\sim 360^{\circ}\text{C}$  for PCPT, and  $\sim 340^{\circ}\text{C}$  for PCPO; see ref. 7). Their heats of fusion are probably also comparable. The cross-sectional area of PCPO exceeds that of the PCPT crystal by 13%. The mismatch at the interface of PCPT crystals would be even greater, since the packing density of PCPO chains in a non-crystalline phase is likely to be lower than in a PCPO crystal. The resulting 'overcrowding' prevents the formation of PCPT crystallites in PCPT-*co*-CPO copolymers with [CPO]  $\geq 0.40$ . In contrast, PCPO crystallites do not suffer from this steric 'overcrowding'.

In the case of PCPT-*co*-CPH copolymers the situation is more complex. The observed melting temperature of PCPH ( $\sim 264^{\circ}\text{C}$ ; see ref. 9) is much lower than that of PCPT; this, in itself, would favour the formation of PCPT crystallites. However, the chain cross-sectional area of PCPH crystals exceeds that of PCPT by  $\sim 9\%$ , i.e. the discrepancy is smaller than in PCPT-*co*-CPO copolymers. The combined effect of these factors results in the observed coexistence of PCPH and PCPT crystallites in PCPT-*co*-CPH copolymers.

For comparison, in poly(*p*-oxybenzoate-*co-p*-phenylene isophthalate)s, where the cross-sectional areas of both crystalline structures are similar, the outcome of crystallization was found to be dependent on copolymer

Table 8 Effect of molar fraction [CPH] of spacer units on wide-angle X-ray diffraction of PCPT-*co*-CPH copolymers in  $2\theta$  range between 10 and  $24^{\circ}$ ; *d*-spacings (nm)

Assignment	[CPH]				
	0	0.25	0.50	0.75	1.00
PCPT peak 1, (0 0 2)	0.628	0.628	0.633	0.633	–
PCPT peak 2, (0 1 0)	0.529	0.509 <sup>a</sup>	0.514 <sup>a</sup>	0.516 <sup>a</sup>	–
PCPT, (1 0 2)	0.495 <sup>a</sup>	–	–	–	–
PCPH peak 1, (2 0 0)	–	0.474	0.471	0.469	0.476
PCPT peak 3, (1 1 0)	0.437	0.441	0.437	–	–
PCPH peak 2, (1 1 0)	–	0.420 <sup>a</sup>	0.416 <sup>a</sup>	0.427	0.425
PCPT peak 4, (2 0 0)	0.394	0.395 <sup>a</sup>	–	–	–
PCPH peak 3	–	–	–	0.380	0.379

<sup>a</sup> Obtained after resolution

composition and, for the 67/33 copolymer, on the crystallization temperature<sup>10</sup>.

## CONCLUSIONS

The crystal structure of the parent rigid-chain 'homopolymer', poly(chloro-1,4-phenylene terephthalate), is similar to that of poly(1,4-phenylene terephthalate), indicating that the presence of a chlorine substituent has little effect on chain packing density.

Poly(chloro-1,4-phenylene 4,4'-oxybisbenzoate), containing an angular ether oxygen atom, has a crystal structure with interchain spacings significantly greater than those of poly(chloro-1,4-phenylene terephthalate). Poly(chloro-1,4-phenylene terephthalate-co-4,4'-oxybisbenzoate) fibres with molar fraction of angular disruptor units [CPO]  $\geq 0.40$ , spun from nematic mesophase at drawdown ratios above 35, were highly oriented and contained crystalline regions consisting of chloro-1,4-phenylene 4,4'-oxybisbenzoate units. The structure of these fibres is not changed significantly by prolonged heat treatments. The chain cross-sectional area of poly(chloro-1,4-phenylene 4,4'-oxybisbenzoate), deduced from the X-ray diffraction patterns of these fibres, exceeds that of the poly(chloro-1,4-phenylene terephthalate) by  $\sim 13\%$ .

The chain packing density in poly(chloro-1,4-phenylene 4,4'-hexamethylenedioxybisbenzoate), containing a flexible spacer, is also lower than in poly(chloro-1,4-phenylene terephthalate). This suggests that the flexible spacer is not fully extended. In contrast to copolymers with the ether oxygen disruptor, those with the hexamethylene flexible spacer have a structure containing crystallites of both parent 'homopolymers'.

Although at this stage there are insufficient data for a rigorous thermodynamic analysis of factors determining the type of crystalline structure or structures to be formed in nematogenic copolymers, the results obtained suggest that the chain cross-sectional areas of the parent homopolymers, together with their melting temperatures, play a significant role.

## ACKNOWLEDGEMENTS

The authors thank Elf (UK) Ltd, Société Nationale Aquitaine (Production) (France) and SERC (Grant GR/D/63110) for financial support.

## REFERENCES

- 1 Dobb, M. G. and McIntyre, J. E. *Adv. Polym. Sci.* 1984, **60/61**, 61
- 2 Kwolek, S. L., Morgan, P. W. and Schaeffgen, J. R. in 'Encyclopedia of Polymer Science and Engineering', Vol. 9, (Eds. H. F. Mark, *et al.*), Wiley, New York, 1987, p. 1
- 3 Jackson, W. J. Jr in 'Contemporary Topics in Polymer Science', Vol. 5, (Ed. E. J. Vandenberg), Plenum Press, New York, 1984, p. 177
- 4 Blackwell, J. and Biswas, A. in 'Developments in Oriented Polymers', Vol. 2, (Ed. I. M. Ward), Elsevier, London, 1987, p. 153
- 5 Mitchell, G. R. and Windle, A. H. in 'Developments in Crystalline Polymers', Vol. 2, (Ed. D. C. Bassett), Elsevier, London, 1988, p. 115
- 6 Krigbaum, W. R., Hakemi, H. and Kotek, R. *Macromolecules* 1985, **18**, 965
- 7 McIntyre, J. E., Maj, P. E. P., Sills, S. A. and Tomka, J. G. *Polymer* 1987, **28**, 1971
- 8 McIntyre, J. E., Maj, P. E. P., Sills, S. A. and Tomka, J. G. *Polymer* 1988, **29**, 1095
- 9 McIntyre, J. E., Maj, P. E. P. and Tomka, J. G. *Polymer* 1989, **30**, 732
- 10 Erdemir, A. B., Johnson, D. J., Karacan, I. and Tomka, J. G. *Polymer* 1988, **29**, 597
- 11 Coulter, P. D., Hanna, S. and Windle, A. H. *Polym. Prepr.* 1989, **30** (2), 49
- 12 Northolt, M. G. *Eur. Polym. J.* 1974, **22**, 965
- 13 Lieser, G. J. *J. Polym. Sci., Polym. Phys. Edn.* 1983, **21**, 1611
- 14 Boon, J. and Magre, E. P. *Makromol. Chem.* 1969, **126**, 130
- 15 Dawson, P. C. and Blundell, D. J. *Polymer* 1980, **21**, 577
- 16 Tabor, B. J., Magre, E. P. and Boon, J. *Eur. Polym. J.* 1971, **7**, 1127
- 17 Wilchinsky, Z. W. in 'Advances in X-ray Analysis', Vol. 6, Plenum Press, New York, 1963, p. 231
- 18 Ungar, G. and Keller, A. *Mol. Cryst. Liquid Cryst. (B)* 1988, **155**, 313
- 19 Leute, V. and Dollhopf, W. *Colloid. Polym. Sci.* 1980, **258**, 353
- 20 Wunderlich, B. 'Macromolecular Physics', Vol. 3, Academic Press, New York, 1980
- 21 Blundell, D. J. *Polymer* 1982, **23**, 359